Experimental study of nonadiabatic core interactions in Rydberg states of calcium

A. Ganesh Vaidyanathan, William P. Spencer, Jan R. Rubbmark, Hajo Kuiper,*
Claude Fabre,† and Daniel Kleppner
Research Laboratory of Electronics and Department of Physics, Massachusetts Institute of Technology, Cambridge, Massachusetts 02139

Theodore W. Ducas
Department of Physics, Wellesley College, Wellesley, Massachusetts 02181
(Received 6 July 1982)

Nonadiabatic contributions to the core polarization in calcium Rydberg states have been investigated experimentally by microwave spectroscopy of F and G states. Transitions $4snf\ ^1F_3 \rightarrow 4sng\ ^1G_4$ have been measured for $n=23-25$. The transition frequencies are in good agreement with calculations based on a dynamical model of the core interaction, but differ by approximately a factor of 2 from the usual adiabatic treatment. The dipole core polarizability of calcium (the polarizability of Ca^+) is found to be $\alpha_1=87(2)$ (atomic units). The quantum defect for the $4sng\ ^1G_4$ series is 0.0310(5). General formulas are presented for the quantum defects of the high-angular-momentum states.

I. INTRODUCTION

For nonpenetrating Rydberg states the major electron-core interaction is due to polarization of the ionic core by the Rydberg electron.[1] In general, core polarization is sensitive to the dynamics of the Rydberg electron. For alkali-metal atoms and other systems with closed-shell cores, a static or adiabatic model of the interaction is usually adequate, and attempts to identify nonadiabatic effects have been inconclusive. For alkaline-earth atoms, however, these effects are expected to be particularly large due to the open-shell nature of the core. Studying them allows us to confirm the dynamical theory of core polarization, to verify calculations of core polarizability and other electron-core interactions, and to make accurate predictions of Rydberg-level structure.

Calcium constitutes an excellent test system for comparing theory and experiment of the nonadiabatic core interactions. The computational problem is simplified by the fact that effects of configuration interactions are small and only a few of the excited states of the ion contribute to the core polarizability. Vaidyanathan and Shorer[2] have calculated the polarization interaction and obtained quantum defects for a number of calcium Rydberg states. The atom is experimentally attractive because the Rydberg states are accessible by excitation with pulsed-dye lasers, and because the quantum defects can be accurately measured by microwave spectroscopy for states in which the calculations are expected to be accurate. In addition, the radiative lifetimes of the Rydberg states of interest vary rapidly with l, providing a simple discriminant for detecting l-changing microwave transitions.

We have measured nonadiabatic contributions to the quantum defects in calcium by high-resolution microwave spectroscopy. An outline of the theoretical method used to calculate the effects is presented in Sec. II, followed by a description of the experimental method and a discussion of the results.

II. THEORY OF NONADIABATIC POLARIZATION EFFECTS

The calculation of the polarization interactions in Ca of Ref. 2 is based on work by Eissa and Öpik.[3] In this section we briefly summarize their theoretical approach. The Hamiltonian for the atom is written

$$H=H_c+H_R+W\ . \tag{1}$$

H_c is the Hamiltonian for the ionic core; H_R is the Hamiltonian for the Rydberg electron in the field of an effective positive point charge of Z-N, where Z is the nuclear charge and N the number of core electrons. The last term

$$W=\sum_{i=1}^{N}\left[\frac{1}{|\vec{R}-\vec{r}_i|}-\frac{1}{R}\right], \tag{2}$$

represents that part of the Rydberg electron-core interaction arising from the finite size of the core. $\vec{R}$

is the position of the Rydberg electron and $\vec{r}_i$ is the position of the ith core electron.

The essence of the Eissa-Öpik method is to treat the residual interaction W as a perturbation of the Hamiltonian $H_0=H_c+H_R$. Energy shifts resulting from this interaction are calculated variationally by using the method of Dalgarno and Lewis.[4] The nonadiabatic contributions arise from inclusion of the dynamical operators of the Rydberg electron in H_R.

The first-order correction to the core wave function Φ^1 is written

$$\Phi^1=\sum_{j=1}^{\infty}\beta_j(R)R^{-j-1}X_j(\hat{R},\vec{r}_i)\ . \tag{3}$$

The summation over j results from the Legendre expansion of the term $1/|\vec{R}-\vec{r}_i|$ in the interaction Hamiltonian W. X_j is the 2^j pole adiabatic distortion corresponding to the first-order correction to the core wave function in the adiabatic model. The term $\beta_j(R)$ is a scaling parameter that is introduced to account for nonadiabatic effects. The functional form of $\beta_j(R)$ is expected to be

$$\beta_j=y_0^{(j)}+y_2^{(j)}/R^2\ , \tag{4}$$

where y_0+y_2 are constants. Minimizing the energy functional through the quadrupole term leads to the following correction to the hydrogenic energy:

$$E^{(2)}=-\tfrac{1}{2}\alpha_1(y_0^{(1)}\langle r^{-4}\rangle+y_2^{(1)}\langle r^{-6}\rangle) -\tfrac{1}{2}\alpha_2(y_0^{(2)}\langle r^{-6}\rangle+y_2^{(2)}\langle r^{-8}\rangle)\ . \tag{5}$$

α_1 and α_2 are the static dipolar and quadrupolar polarizabilities of the core, respectively. In the limit that $y_0^{(j)}\to 1$ and $y_2^{(j)}\to 0$, Eq. (5) reduces to the usual adiabatic result

$$E^{(2)}=-\tfrac{1}{2}\alpha_1\langle r^{-4}\rangle-\tfrac{1}{2}\alpha_2\langle r^{-6}\rangle\ . \tag{6}$$

The polarizabilities and coefficients $y_i^{(j)}$ have been calculated for $l=3-6$ by Vaidyanathan and Shorer.[2] These results are presented in Table I.

TABLE I. Polarizabilities and y coefficients for calcium, from Ref. 2.

	Dipole polarizability $\alpha_1=89(9)$ Quadrupole polarizability $\alpha_2=987(90)$			
l	$y_0^{(1)}$	$y_2^{(1)}$	$y_0^{(2)}$	$y_2^{(2)}$
3	0.76	−4.48	0.37	−2.37
4	0.80	−0.56	0.33	−0.01
5	0.98	−16.60	0.66	−1.45
6	1.02	−33.70	0.91	−30.81

The contribution to the quantum defect due to the polarization interaction is related to $E^{(2)}$ by

$$E^{(2)}=-\frac{1}{2}\left[\frac{1}{(n-\delta_p)^2}-\frac{1}{n^2}\right]\simeq\frac{\delta_p}{n^3}\ . \tag{7}$$

A. Contributions to the quantum defects

As discussed in Ref. 2, the total quantum defect of a nonpenetrating Rydberg state can be written

$$\delta_l=\delta_p+\delta_{\rm pen}+\delta_{\rm rel}+\delta_{ci}+\delta_{\rm ret}\ . \tag{8}$$

δ_p represents the effects of the polarization interaction. $\delta_{\rm pen}$ describes the effects of penetration of the Rydberg electron into the core; it is assumed to be small. $\delta_{\rm rel}$ and $\delta_{\rm ret}$ represent relativistic and retardation effects, respectively, and δ_{ci} describes the effects of a possible configuration interaction between the Rydberg state and valence states.

For nonpenetrating states the quantum defect is dominated by δ_p. It is convenient to distinguish the dipole and quadrupole contributions. Writing $\delta_p=\delta_{p1}+\delta_{p2}$, Eqs. (5) and (7) yield

$$\delta_{p1}=\tfrac{1}{2}n^3\alpha_1(y_0^{(1)}\langle r^{-4}\rangle+y_2^{(1)}\langle r^{-6}\rangle)\ ,$$
$$\delta_{p2}=\tfrac{1}{2}n^3\alpha_2(y_0^{(2)}\langle r^{-6}\rangle+y_2^{(2)}\langle r^{-8}\rangle)\ . \tag{9}$$

To extract α_1 from spectroscopic measurements of the quantum defects we use

$$\alpha_1=\frac{2}{n^3(y_0^{(1)}\langle r^{-4}\rangle+y_2^{(1)}\langle r^{-6}\rangle)}(\delta_l-\delta_l')\ , \tag{10}$$

where δ_l' represents contributions to the quantum defect arising from everything but the dipolar polarization term in Eq. (8).

B. Comparison with experiment

The quantum defect of the G state δ_G is used to compare the dynamical theory with experiment. For $l<4$ the quantum defects cannot be calculated reliably due to effects of core penetration and configuration interaction, while for $l>4$ the dynamical terms become relatively less important. The measured quantity is the transition frequency between singlet states of identical n and different l: $l=3\to l=4$. Because δ_F is known independently from spectroscopic data,[5] the measurement yields the absolute value of δ_G.

The transition frequencies ν_n are related to the quantum defects δ_F and δ_G according to

$$\nu_n = c\mathcal{R}\left[\frac{1}{(n-\delta_F)^2}-\frac{1}{(n-\delta_G)^2}\right], \tag{11}$$

which yields

$$\delta_G = n-\frac{(n-\delta_F)}{[1-(n-\delta_F)^2\nu_n/c\mathcal{R}]^{1/2}}. \tag{12}$$

III. LIFETIMES OF CALCIUM ^1F AND ^1G SERIES

Because the $4snf$ and $4sng$ states have almost identical field-ionization thresholds they cannot be distinguished easily by selective field-ionization techniques. Instead, we made use of the variation with l of radiative lifetimes. This method, which was previously employed in cesium by Safinya, Gallagher, and Sandner,[6] is particularly well adapted to calcium because the ^1F lifetimes are approximately a factor of 10 shorter than the ^1G lifetimes.

To calculate the ^1G state lifetimes we employed the Coulomb matrix element routine of Zimmerman *et al.*[7] Core contributions to the matrix elements were taken into account using the Hartree-Slater theory. For the $4s\,25g\ ^1G$ state the result was $\tau=24$ μsec. For $n>10$ the calculated lifetimes fit the following scaling law: $\tau=1.81(n^*)^{2.95}$ nsec.

When a similar calculation was carried out for ^1F states, the lifetime for $n=25$ was found to be 1.6 μsec. Such a calculation is unreliable, however, because it neglects configuration interactions in the ^1D series. An accurate calculation could be carried out within the framework of multichannel quantum-defect theory,[8] but we opted to measure the lifetime directly. For the $4s\,25f\ ^1F$ state, we obtained $\tau\simeq 2.5(5)$ μsec. The factor of 10 between the ^1F and ^1G series is sufficient to allow them to be clearly distinguished experimentally.

IV. EXPERIMENT

The measurements were conducted on an effusive beam of calcium atoms within an interaction region cooled to 77 K. Details of the apparatus are described in Ref. 9. The interaction region is surrounded by a mumetal shield to eliminate effects of the ambient magnetic field. The atoms are excited to the state $4snf\ ^1F$ by two pulsed-dye lasers. The first step excites the transition $4s^2\ ^1S\rightarrow 4s4p\ ^1P$ (423 nm). The second step (393 nm) excites a $P\rightarrow F$ transition via Stark mixing between the ^1F and ^1D series. The states $4snf\ ^1F$ are almost degenerate with states $4s(n+1)d\ ^1D$ for $n\simeq 25$.[5] By applying a small electric field ($\sim$20 V/cm) during the laser pulse, the ^1F states can be excited. The transition $4snf\ ^1F-4sng\ ^1G$ is then excited by microwave radiation at approximately 30 GHz. The Rydberg atoms are detected by application of an ionizing field. The ions pass through small holes in one of the field plates to an electron multiplier. The field-ionizing pulse is delayed with respect to the laser pulse by 25 μsec, at which time the ^1F atoms have essentially completely decayed.

The microwave source is a HP 8690B sweep oscillator that is synchronized to a harmonic of a stabilized HP 606B reference oscillator operating at approximately 55 MHz. A small fraction of the microwave power is diverted to a calibrated wave meter to determine the correct harmonic.

The natural linewidth for the transition is governed by the ^1F lifetime. The optimal spectral resolution is achieved when the pulse length of the applied microwave field is approximately equal to this lifetime: shorter time gives undesirable broadening, while longer time causes loss of signal due to decay through the ^1F state. For this reason it is imperative that the microwave interaction time be strictly limited. This was achieved by a gating circuit set to a 1.6-μsec aperture. An overall timing diagram is shown in Fig. 1.

The natural resonance line shape is a somewhat complicated function that combines features of a Lorentzian line and a Rabi resonance curve. The full width at half maximum is estimated to be 560 kHz. A typical resonance for the transition $4s\,25f\ ^1F\rightarrow 4s\,25g\ ^1G$ is shown in Fig. 2. The linewidth, typically 1 MHz, is attributed primarily to inhomogeneities in the ambient electric field.

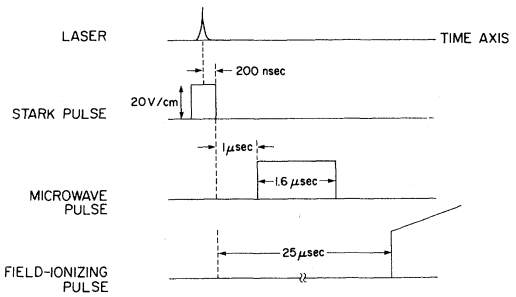

FIG. 1. Timing diagram for the experiment: Stark pulse is used to access the F state, microwave pulse to drive the $F\rightarrow G$ transition, and field-ionizing pulse to detect the G state.

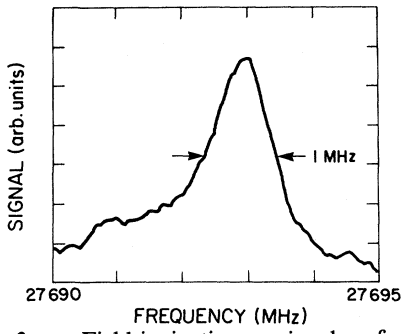

FIG. 2. Field-ionization signal for the $4s\,25f\,{}^1F_3 \rightarrow 4s\,25g\,{}^1G_4$ transition in calcium.

The high l states are extremely sensitive to such fields. A gradient of 10^{-3} V/cm^2 accounts for the observed broadening. Such a gradient is entirely possible under the experimental conditions. Other sources of linewidths—power broadening, Doppler broadening, frequency jitter, etc.,—are believed to be negligible. The uncertainty in the transition frequencies, typically 100 kHz, is due to asymmetries in the lineshape arising from the field gradients.

V. RESULTS

Final experimental values for transitions ${}^1F \rightarrow {}^1G$, $n=23-25$, are given in Table II. Theoretical values from the adiabatic and dynamical calculations are also shown. The experimental values agree with the prediction of the dynamical theory to within the accuracy of the calculations. It should be emphasized that the theory contains no adjustable parameters: The uncertainty arises from the *ab initio* calculation of the core polarizability. In contrast, predictions of the adiabatic model are in serious error, approximately a factor of 2.

The best value of the δ_G can be obtained by combining our microwave measurements with spectroscopic data on δ_F, using Eq. (12). As described in Ref. 2, optical data by Borgström and Rubbmark[5] yield, for $n=23-25$,

$$\delta_F = 9.61(5) \times 10^{-2} . \tag{13}$$

The results for δ_G are shown in Table III.

The G-state quantum defect can be analyzed to yield a value for the dipole core polarizability of calcium. To accomplish this the nondipolar contributions to the quantum defect must be evaluated. Table IV, from Ref. 2, reveals that these are so small that δ_G is essentially determined by δ_{p1}. With the use of Eq. (10), and the calculated value of y_0^1 and y_0^2 from Table I, the experimental value of α_1 is obtained as shown in Table III. The final result is $\alpha_1 = 87(2)$ a.u. The major source of error is uncertainty in α_2 from Ref. 2. This result for α_1 is in excellent agreement with the theoretical value of Vaidyanathan and Shorer, [89(9)].

For states with $l > 4$, the quantum defects are dominated by the polarization interaction. These quantum defects can be calculated reliably from Eq. (9) by combining the measured dipole polarizability $\alpha_1 = 87(2)$, the theoretical values of α_2 and the y parameters presented in Table I, and hydrogenic values for $\langle r^{-n} \rangle$. (Expressions for the latter are given in Ref. 10.) For $l > 6$ the adiabatic dipole term dominates and

$$\delta \simeq (3/4)\alpha_1 / l^5 = 65.3/l^5 .$$

This result, which is accurate to 2%, applies to singlet states and also to triplet states provided that fine structure is taken into account. As explained in Ref. 1, the corrections for fine structure are unimportant except for very high l states.

TABLE II. Measured transition frequencies in calcium compared with predictions of adiabatic and dynamical models. The larger uncertainty for the $4s\,23f\,{}^1F_3 \rightarrow 4s\,23g\,{}^1G_4$ transition was due to difficulties locking the sweep oscillator at this frequency.

Transition	Expt. (GHz)	Dynamical Model (GHz)	Adiabatic Model (GHz)
$4s\,23f \rightarrow 4s\,23g$	35.4626(5)	32.3(40)	72.3(70)
$4s\,24f \rightarrow 4s\,24g$	31.2513(1)	28.5(30)	63.7(60)
$4s\,25f \rightarrow 4s\,25g$	27.6926(1)	25.2(30)	56.4(50)

TABLE III. Values for the G quantum defect δ_G, and the dipole core polarizability α_1 derived from the microwave data shown in Table II.

n	δ_G	α_1
23	$3.09(8) \times 10^{-2}$	87(3)
24	$3.10(8) \times 10^{-2}$	87(3)
25	$3.10(8) \times 10^{-2}$	87(3)

TABLE IV. Nondipolar contributions to the quantum defect of the $4s\,25g\,{}^1G_4$ state. These contributions were estimated using numerical procedures discussed in Ref. 2.

Level	δ_{quad}	δ_{pen}	δ_{rel}	δ_{ret}
$4s\,25g\,{}^1G_4$	1.4×10^{-3}	2.0×10^{-5}	5.9×10^{-6}	-6.4×10^{-7}

ACKNOWLEDGMENTS

This work was supported by the Office of Naval Research Contract No. N0014-7900813. H. Kuiper was supported by a Fulbright travel grant and by the Deutsche Forschungsmeinschaft; C. Fabre was supported by the CNRS. We are grateful to Randall G. Hulet for developing the stabilized microwave system used in this work and to Michael M. Kash for useful discussions.

---

*Present address: Physikalisches Institut der Universitat Erlangen-Nurnberg, Erwin-Rommel-Strasse 1 D-8520 Erlangen, Federal Republic of Germany.

†Present address: Laboratoire de Physique de l'Ecole Normale Superieure, 24 rue Lhomond, 75231 Paris Cedex 05, France.

[1]R. R. Freeman and D. Kleppner, Phys. Rev. A 14, 1614 (1976).

[2]A. G. Vaidyanathan and P. Shorer, Phys. Rev. A 25, 3108 (1982).

[3]H. Eissa and U. Öpik, Proc. Phys. Soc. London 92, 556 (1960).

[4]A. Dalgarno and J. T. Lewis, Proc. R. Soc. London, Ser. A 233, 70 (1955).

[5]S. A. Borgström and J. R. Rubbmark, J. Phys. B 10, 18 (1977).

[6]K. A. Safinya, T. F. Gallagher, and W. Sandner, Phys. Rev. A 22, 6 (1980).

[7]M. L. Zimmerman, M. G. Littman, M. M. Kash, and D. Kleppner, Phys. Rev. A 20, 6 2251 (1970).

[8]M. Aymar, R. J. Champeau, C. Debart, and J. C. Keller, J. Phys. B 14, 4489 (1981).

[9]W. P. Spencer, A. G. Vaidyanathan, D. Kleppner, and T. W. Ducas, Phys. Rev. A 25, 380 (1982).

[10]K. Bocasten, Phys. Rev. A 9, 1087 (1974).